Influence of porous media on carbon dioxide hydrate formation and dissociation processes by calorimetry for secondary refrigeration applications

Pascal Clain, Fatima Doria Benmesbah, Olivia Fandino, Véronique Osswald, L. Fournaison, Christophe Dicharry, Livio Ruffine, Anthony Delahaye

DOI: 10.18462/iir.icr.2023.0263

Influence of porous media on carbon dioxide hydrate formation and dissociation processes by calorimetry for secondary refrigeration applications.

Pascal CLAIN*[(a, b)], Fatima Doria BENMESBAH[(b, c)], Olivia FANDINO[(c)], Veronique OSSWALD[(b)], Laurence FOURNAISON[(b)], Christophe DICHARRY[(d)], Livio RUFFINE[(c)], Anthony DELAHAYE[(b)]

[(a)] Leonard de Vinci Pôle Universitaire, Research Center
Paris La Défense, 92916 France
[(b)] Université Paris-Saclay, INRAE, FRISE,
Antony, 92761, France.
[(c)] Geo-Ocean, Univ Brest, CNRS, Ifremer, UMR6538,
Plouzane, F-29280, France
[(d)] CNRS/TOTALENERGIES/UNIV PAU & PAYS ADOUR, Laboratoire des Fluides Complexes et leurs Réservoirs - IPRA, UMR5150
Pau, 64000, France

ABSTRACT

Understanding the formation and dissociation mechanisms of gas hydrate in porous media is important for the development of new technologies related to cold storage as they provide significant latent heat and energy density at suitable phase change temperature. In this work, we investigated CO2 hydrate formation and dissociation in two different porous materials: sand and silica gels. A calorimetric approach is applied to study both the CO2 hydrate formation kinetics, particularly the induction time, and the amount of hydrate formed in both porous materials. The present work is focused on assessing the effect of key factors like water saturation, particle size and the morphology of porous media on CO2 hydrate formation and dissociation processes. Interestingly, the results obtained with mesoporous silica gel showed a higher amount of hydrate formed compared to those with sand for similar initial pressure, temperature and water content conditions.

Keywords: CO2 hydrate, Cold storage, Differential thermal analysis, Particle and Pore size, Water saturation

1. INTRODUCTION

The development of a cost-effective and environmentally friendly secondary refrigeration system requires a good balance between energy demand and supply. In this context, the cooling capacity of the system has to be sufficient during peak hours when energy consumption is high. Cold storage is a suitable method to increase this cooling capacity. The challenge of this technology is to select a refrigerant with high energy density and high heat transfer capacity in order to reduce the system power consumption. Gas hydrates have attracted the attention of several researchers who considered them as a potential candidate due to their interesting thermodynamic properties. They are stable over a wide range of temperatures (in particular for T > 273 K, for example, CO2 hydrates can form at a rough range of temperatures between 273 and 283 K, and an approximate pressure range of 1.5-4.5 MPa), which is of a particular interest for air conditioning (Fournaison et al., 2004; Li et al., 2012). According to a recent review of literature enhancing mass transfer

by forming CO2 hydrates in porous media could improve Cold Thermal Energy Storage (CTES) design (Wang et al., 2020). However, related current research is focused on other applications such as gas separation, CO2 sequestration (Oya et al., 2017), and mainly on understanding natural hydrate dynamics (Malagar et al., 2019). To our knowledge, very few studies have been published on the use of porous media in CO2 hydrate-based cold storage technologies. More recently, Cheng et al. (2020) reported on the use of porous media as a hydrate reinforcement method aiming at reducing the induction time of hydrate formation, increasing nucleation rates, and bettering the cold storage density of the cold storage media. In addition, as mentioned previously Wang et al. (2020) pointed out in a review that one of the important challenges of CTES systems based on CO2 hydrates is a low mass transfer due to limited gas-liquid interface. The authors suggested the use of porous media in future work to improve mass transfer and thus the gas-liquid interface.

In order to provide a large surface area and potentially to limit energy consumption related to the stirring required in bulk media, the present paper seeks to address CO2 hydrates formation and dissociation in porous media using a calorimetric approach. The effect of key factors such as water saturation, particle size and the morphology of the porous media on the solid mass fraction formed was investigated.

2. MATERIALS AND METHODS

2.1. Materials

Carbon dioxide with a certified purity of more than 99.7 % was supplied by Linde Gas (France). Fontainebleau silica sand purchased from Laboratoires Humeau (La Chapelle-sur-Erdre, France) and spherical silica porous gel particles of nominal pore diameters of 30 and 100 nm supplied by Silicycle Co. (Canada) were used as porous media. All materials were used without further purification. The detailed properties of silica sand and silica gel are listed in Table 1.

Table 1: Physical properties of Fontainebleau silica sand and silica gel samples

Parameters	Fontainebleau silica sand	30 nm Silica gel	100 nm Silica gel
Mean particle diameter (µm)	80-450	20-45	20-45
Mean pore diameter (nm)	-	30	100
Pore volume ($cm^3.g^{-1}$)	-	0.86	0.7
Dry density ($g.cm^{-3}$)	2.65	2.2	2.2

To study the influence of particle size on CO2 hydrate formation and dissociation, Fontainebleau silica sand was sieved to 3 classes of particles: 80 to 160 µm; 160 to 315 µm and 315 to 450 µm noted respectively PS01, PS02 and PS03.

2.2. Differential thermal analysis (DTA) apparatus description

A differential thermal analysis (DTA) apparatus was used for the experiments, whose principle was described in a previous work (Fournaison et al., 2004). It was designed to measure the difference in thermal behaviour between two identical cells submitted to the same heat flux. A schematic diagram of the experimental apparatus is shown in Figure 1. It consists of two identical and symmetric transparent glass cells with a functional volume of 40 ml. The transparent walls enable visualization of the studied samples inside the cells.

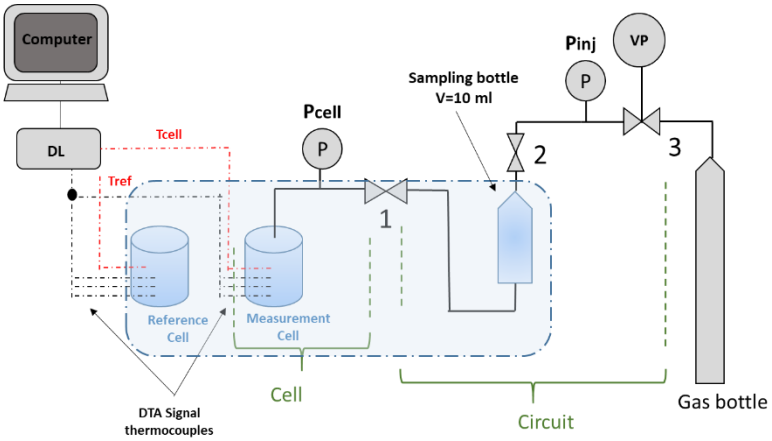

Figure 1: Schematic diagram of the DTA experimental apparatus. (DL) Data logger, (P) Pressure transducer, (Tcell, Tref) Thermocouple to measure direct temperature, (VP) Vacuum pump, the blue area corresponds to a temperature-controlled bath in which the two cells are immersed, as well as the sampling cylinder

The two cells are immersed in a temperature-controlled bath (blue area in Figure 1). One of them is filled with the porous media at a certain water saturation and used as the reactor for hydrate formation (called measurement cell). The second cell (called reference cell) is filled with the same porous media and water saturation as the measurement cell with an inert solution of water-ethanol 50 % vol/vol, in order to avoid crystallization during the thermal cycle while having thermal properties close to those of the liquid in the measurement cell. Each cell is equipped with one thermocouple that gives a direct temperature measurement (±0.5 K). The DTA measurement is based on the use of six thermocouples, three of which are inserted in one cell and three in the other. These six thermocouples are connected together in series, by a back and forth connection between the two cells. The back and forth connection allow to amplify the differential signal between the two cells, while limiting the error to one measurement, i.e. the signal recovered by the acquisition unit.

2.3. Experimental procedure: DTA analysis of CO2 hydrate formation and dissociation in silica sand

After pressurizing the measurement cell with CO2 using an expansion method to the desired experimental pressure set around 2.5 MPa, the bath temperature was then set to 285.15 K to stabilize the temperature inside both cells at an initial equilibrium state. After the initial equilibrium state, the system was gradually cooled down until 271.15 K.

The temperature peak (red line) indicates CO2 hydrate formation due to the exothermic property of crystallization. Meanwhile, the DTA signal peak (blue line) illustrates the difference in heat transfer between the two cells. When the exothermic reaction occurs in the measurement cell, the DTA signal increases rapidly with a similar pattern compared to the direct measurement of the temperature. CO2 hydrate formation is also accompanied with a temperature peak and a strong decrease in the system pressure due to the consumption of CO2 during the hydrate growth. Figure 2a shows the presence of two consecutive DTA peaks (2 red arrows on Figure 2a). These two peaks are accompanied with 2 consecutive pressure drops corresponding to gas consumption by hydrates. This result suggests the occurrence of multiple nucleation followed by growth of CO2 hydrates in silica sand. When pressure, temperature and DTA signal stabilized the thermodynamic equilibrium was considered to be reached, and CO2 hydrate formation finished. Hydrate dissociation was triggered by increasing the bath temperature gradually with a rate of 0.1 $K.min^{-1}$ until the initial temperature was reached (285.15 K). As shown in Figure 2b, hydrate dissociation is expressed by a large and opposite variation in the DTA signal compared to hydrate formation. This is due to the endothermic nature of hydrate dissociation. The discretization of the DTA signal obtained during hydrate dissociation was performed to determine the experimental dissociation enthalpy and calculate the mass of hydrates formed in the reactor.

a)

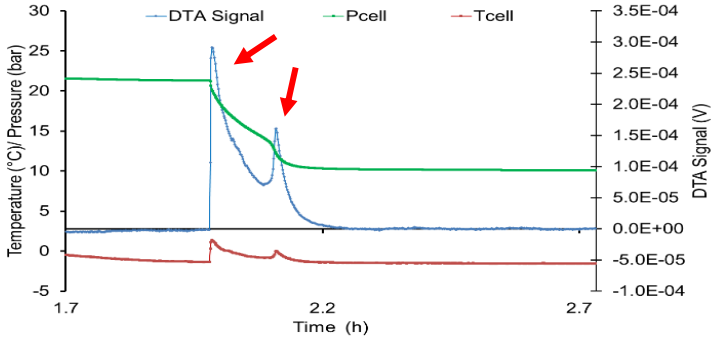

b)

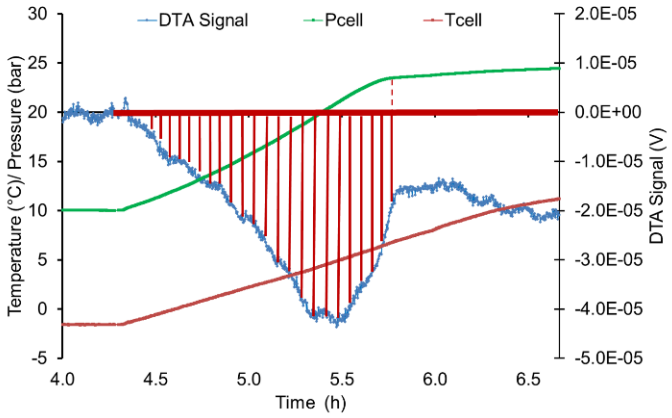

Figure 2: Temperature, pressure and DTA signal profiles during CO2 hydrate formation and dissociation in silica sand at 33 % water saturation. Figures a) and b) focus on CO2 hydrates formation peak and CO2 hydrates dissociation peak respectively.

3. RESULTS

3.1. Impact on amount of hydrates formed

3.1.1. Effect of water saturation

The influence of water saturation on the mass of gas hydrates formed was first investigated based on a set of experiments on silica sand with various water saturation conditions and particle size. Table 2 summarizes the experimental conditions applied to this set of experiments and the final water to hydrate conversion (based on the fixed hydration number of CO2 hydrate).

Table 2: CO2 hydrate formation and dissociation results in a sandy matrix for several water saturations and particle size

Run	Sample state (F: fresh sample. M: memory sample)	Particle size (µm)	Water saturation (%)	Mass of hydrates formed (g)	Water conversion to hydrate (%)
1	F	Non-sieved sand	33.4	3.17	41.2
2	F		52.0	3.39	28.1
3	F		59.9	3.20	21.8
4	F		63.7	1.87	12.5
5	M		63.7	2.27	14.9
6	F		75.2	2.16	12.3
7	F		100	No hydrate formation succeeded	
8	F	PS01	53.4	4.47	32.3
9	F	PS02	51.5	3.60	28.7
10	F	PS03	51.8	3.16	25.7

The influence of water saturation on the amount of hydrates formed is also represented in Figure 3, with the mass of the hydrate formed and the rate of water to hydrate conversion as a function of water saturation of non-sieved silica sand. It is interesting to note that the amount of hydrates formed is not significantly different for water saturations ranging from 33 to 60 %. However, for higher water saturation (63 % and higher), the results show lower values of the mass of hydrates formed. It is also interesting to note that the rates of water conversion to hydrates are between 12 and 41 % and follow a decreasing tendency with the increase of water saturation. This is due to the fact that in the measurement cell the formation of hydrates takes place in a closed system after CO2 injection. In fact, the gas first dissolves in water under temperature conditions outside the hydrate stability zone. After reaching a stable saturation, which corresponds to the same (P, T) conditions for all experiments, the system is closed. Thus, knowing that the density of CO2 in vapor phase is higher than the density of CO2 dissolved in liquid phase, the total amount of CO2 in the system also decreases when increasing water saturation. With less CO2 available in the system, and more water, then less hydrate is formed, as confirmed by the results from a previous solid fraction model based on an equilibrium balance on CO2 in its different vapor, dissolved in liquid and hydrate phases (Marinhas et al., 2007). It is interesting to note that these mass balance results are in the same range of values as the present results from the calorimetric approach as seen in Figure 3 with the open and full green diamonds.

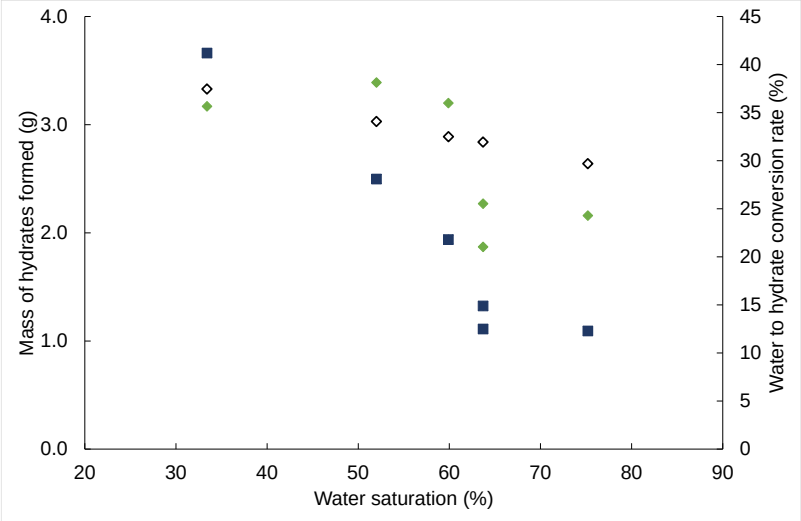

Figure 3: Mass of hydrate formed (◆: present calorimetric approach; ◇: previous mass balance approach (Marinhas et al., 2007) and water to hydrate conversion rate (■) as a function of water saturation of silica sand.

Overall, these findings confirm the existence of a strong correlation between water saturation and the amount of CO2 hydrate formed, as it is reported in previous studies for CH4 hydrates in several porous media (Ge et al., 2019; Pan et al., 2018). As the focus of this study is to appreciate optimal water saturation conditions for an efficient cold storage system, the results demonstrate that a 50-60 % water saturated system could be a suitable level to maximize the amount of energy stored. This optimal saturation value is slightly lower than the value usually used in the literature to improve hydrate formation kinetics around 70 % (Ge et al., 2019; Mekala et al., 2014).

3.1.2. Effect of particle size

For the study of the effect of particle size on CO2 hydrate formation and dissociation in porous media, Fontainebleau silica sand was sieved into 3 particle size classes: PS01, PS02 and PS03. The pore volume for the particle size classes being the same, the same quantity of water is used in the various sand samples. A clear decreasing tendency of the amount of hydrate mass and hydrate conversion rate as a function of the four particle size classes is observed in Table 2. This pattern is due to the decrease of the specific area resulting from the increase of particle size. Indeed, for a larger specific area (smaller particle size) water is adsorbed on a larger surface area. This could potentially enhance the liquid-gas contact area, which can improve gas hydrate formation. This suggests that CO2 hydrate formation occurs preferentially at the solid-liquid interfaces of sand particles. It is important to note that the mass of hydrates obtained within the non-sieved sand is close to the amount within PS02 because this class represents 80 % of the non-sieved sand. Alternatively, it is possible to assume that the fraction leftover representing 10 % has no significant influence on the hydrate conversion rate.

These findings are consistent with some previous studies reported in the literature (Ge et al., 2019; Mekala et al., 2014; Qin et al., 2022) and mentioned in the introduction section. However, other studies demonstrated an opposite result (Kumar et al., 2015; Pan et al., 2018). In this case, it has been suggested, globally, that hydrates formed in smaller pores may obstruct gas diffusion in the porous media. In their recent review Qin et al. (2021) also reported this inconsistency between previous studies on the influence of particle size on hydrate formation. Indeed, the authors suggested that this discrepancy in the results of the above-mentioned studies might be due to the influence of other factors, such as the initial water saturation used in each study, the composition of the gas phase, the specific surface area, or even the experimental system and hydrate formation procedure used.

3.1.3. Effect of the morphology

In this section, results from the investigation of CO2 hydrate formation and dissociation in two morphologically different porous media, silica sand and silica gel, are reported. Fontainebleau silica sand is considered as a uniform grain size structure (with only external porosity) and silica gel as a dual porosity media (with internal and external porosity). The data of mass hydrate formed and water to hydrate conversion rates are illustrated in Table 3.

Table 3: CO2 hydrate formation and dissociation results in silica gel

Run	Pore size (nm)	Water saturation of Pore volume Sw_p (%)	Water saturation of Interstitial space Sw_i (%)	Induction time (min)	Mass of hydrate formed (g)	Water to hydrate conversion rate (%)	Induction time (min)	Driving force (% mol CO_2/mol H_2O)
1	100	53	0	No hydrate				
2		78	0	165	4.63	38.4	165	0.50
3		100	0	203	4.70	30.9	203	0.80

4		100	0	102	4.83	32.8	102	0.89
5		100	32	82	2.68	11.1	82	0.77
6	30	100	0	100	4.52	24.0	100	0.77
7		100	30	740	5.02	19.3	740	0.92
8		100	43	253	2.45	8.4	253	0.78

The results of hydrate mass formed and water to hydrate conversion rates are shown in Table 3 and Figure 4. Globally, it can be seen from Figure 4 that the water to hydrate conversion rates in silica gel, as well as hydrate mass, are higher in comparison with silica sand. Regarding water to hydrate conversion rate, the results show a decreasing tendency when the initial amount of water increase in the system. As it is observed in silica sand, when the amount of water in silica gel increases, it results in a decrease in the amount of CO2 initially injected in the measurement cell of the DTA apparatus. Furthermore, when the amount of water introduced in silica gel is sufficient to saturate not only the pore volume but also the interstitial space, the system configuration is closed to that obtained in silica sand and the amount of hydrate formed are comparable in some cases (points marked with red circles in Figure 15). In this case, the formation of hydrate could be affected by the heterogeneous distribution of water and gas in the porous media. This can explain the decrease in the amount of hydrate formed observed with both pore size of silica gel (100 nm and 30 nm)

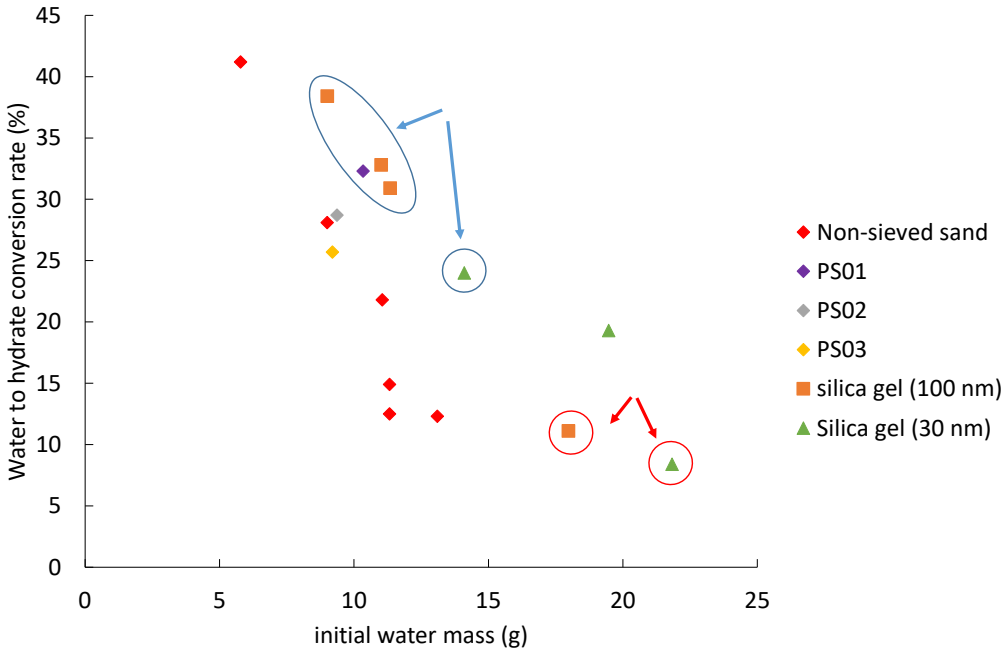

Figure 4: Water to hydrate conversion rate as a function of initial water content.

3.2. Impact on induction time

3.2.1. Effect of water saturation

The influence of water saturation on induction time was first investigated based on a set of experiments on silica sand with various water saturation conditions and particle size. Figure 5 shows the induction time values obtained as a function of water saturation of the porous sample in the cell. The induction time is defined as the time difference between the moment when theoretical thermodynamic equilibrium is reached for hydrate formation and the moment when supercooling breaks down. To our knowledge, induction time data for CO2 hydrates as a function of water saturation of the porous media are poorly known. The induction time

values are scattered and vary between 51 and 120 min for the majority of the experiments except for Sahu et al. (2022). They showed an important induction time of 2083.8 min within a silica sand of 0.15 mm particle diameter at 70 % water saturation. The induction time dispersion may be due to several key factors such as the configuration of the experimental system (reactor type and design, the internal volume, operating conditions, driving force…). There are therefore biases of interpretation when different works are compared. A slight increase of induction time can be observed when water saturation of silica sand increases. However, for the repeated experiment at 63.7 % water saturation (Run 5), it can be noted a considerable difference in the induction time compared to the rest of the experiments. This discrepancy in induction time may be related to a heterogeneous redistribution of the water within the porous media after hydrate dissociation. Indeed, the CO2 hydrate formation experiments in this study are performed for an experimental temperature of 271.15 K and under pressure conditions around 2.5 MPa. In Table 3 we reporter the driving force for each run. The latter is calculated using the method reported by Boufares et al. (2018). It is interesting to note that a slight increase of the driving force does not have a significant influence on induction time. The latter increases slightly but the vast majority of the data remains in a narrow range.

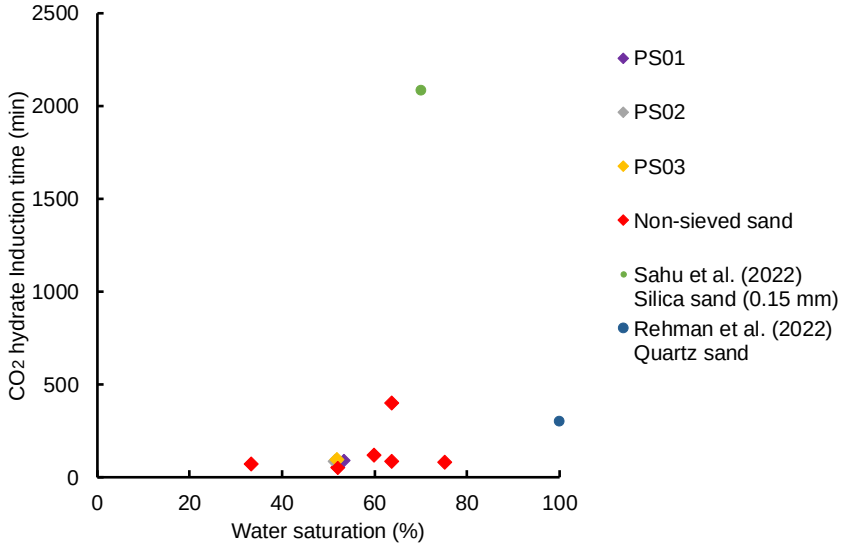

Figure 5: Induction time as a function of water saturation of silica sand and particles size

3.2.2. Effect of particle size

It is well known that pore size is one of the main parameters determining hydrate formation kinetic in porous media. Table 3 showed that the induction time values at which CO2 hydrate formation is detected for the 3-particle size classes are relatively homogeneous with an average value of 87±5 min. They present a difference of 35±5 min compared to the induction time obtained for non-sieved silica sand as shown on Table 3. Overall, it is difficult to establish from these results an obvious correlation between induction time and particle size of silica sand. The results reported in the literature seem to diverge regarding the effect of particle size on induction time. As observed by Qin et al. (2021), some studies demonstrated a positive effect of small particle size on shortening the induction time (Heeschen et al., 2016; Zhang et al., 2018). This may be due to a larger nucleation area when decreasing particle size. However, other studies found an opposite effect even though a similar particle size and porous media were used (Liu et al., 2015; Qin et al., 2021). Qin et al. (2021) suggested that the reason for this divergence is related to the fact that induction time is strongly affected by many other factors like: (1) the experimental method used to form hydrate, (2) the geometry of the experimental device, (3) the type of hydrate formed, etc. This could also explain the results obtained in this study.

3.2.3. Effect of the morphology

It is well known that the driving force, necessary to initiate the formation of hydrates in silica gels, increases when the pore sizes decrease because the thermodynamic equilibrium conditions are more difficult to reach.

Therefore, at constant driving force, when the pore sizes decrease the induction time must increase. This can be seen in Table 3 where for a driving force around 0.8 %mol CO2/molH2O, the induction time increases up to 25 % in 30 nm silica gels compared to 100 nm. Figure 6 gathers the result obtained for silica gel and silica sand as a function of the initial water mass introduced in the porous media. It can be seen that induction time values for the experiments performed in silica gel are quite scattered between 82 and 235 min. A significant difference in the induction times was noted in the case of silica gel with an internal pore size of 30 nm, and a water saturation of the pore volume and the interstitial space (Run 7, ≈740 min). In addition, it can notice that for a similar initial water content, the induction time values obtained for silica gel are close, and slightly higher in some cases, than those obtained in Fontainebleau silica sand. For high water content, particularly in the case of 30 nm pore (Run 7 and 8) size silica gel, the induction time values are higher than in the case of low water content (Run 6). Knowing that for these two particular experiments, water occupies both the pore volume and the interstitial space, this points to the hypothesis that water-gas contact is hindered by the presence of water in the interstitial space.

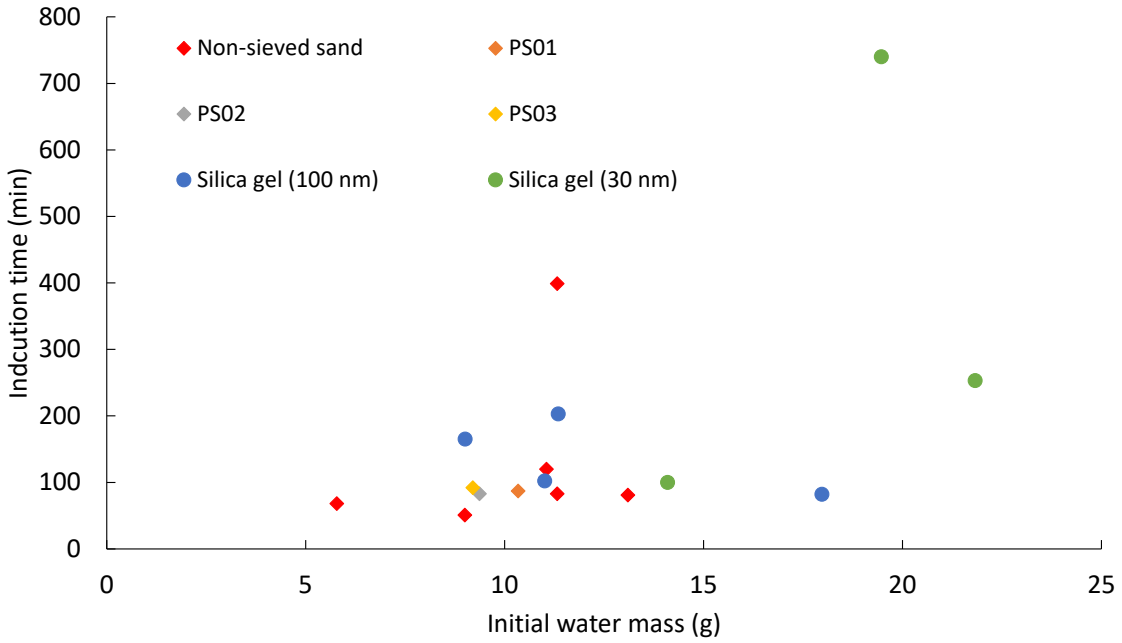

Figure 6: Induction time in silica sand, 100 nm silica gel and 30 nm silica gel as a function of initial water content.

Consequently, it is difficult to draw conclusions, given that hydrate nucleation is a stochastic process. Furthermore, when water saturates partially the pore volume (Swp = 53 %) which corresponds to an initial water content of 0.37 (correspond to an initial water mass of 6 g) (Run 1), gas hydrate formation was not detected (no DTA signal related to hydrate formation, and no pressure and temperature variation). This may be due to the adsorption of water on the internal pore surface of silica gel, which makes the amount of free water not sufficient for hydrate formation.

4. CONCLUSION

The influence of key factors related to the use of porous media on CO2 hydrates formation and dissociation processes the effect of water saturation, particle size and the morphology of the porous media on induction time, storage capacity and equilibrium conditions on the solid mass fraction formed and the induction time was investigated:

- For water saturation, the analysis of the results obtained with silica sand did not reveal a noteworthy effect on the induction time. Furthermore, when water saturation increases in a closed system and for the

same initial pressure condition, the amount of CO2 initially injected in the cell decreases, which results in a lower mass of hydrates formed, and thus, a lower water to hydrate conversion rates.

- For particle size, within silica sand, it has shown that this factor does not influence the induction time, whereas, the results indicated a strong effect on the amount of hydrate formed. Indeed, for a smaller particle size, liquid-gas contact area is enhanced due to water adsorption on a larger surface area. This can potentially enhance the amount of hydrate formed.

- Finally, the results showed a higher amount of thermal energy stored by hydrates formed in silica gel compared to Fontainebleau silica sand. Moreover, a configuration where water occupies only the pore volume of silica gel was found to be optimal.

REFERENCES

Boufares, A., Provost, E., Dalmazzone, D., Osswald, V., Clain, P., Delahaye, A., Fournaison, L., 2018. Kinetic study of CO2 hydrates crystallization: Characterization using FTIR/ATR spectroscopy and contribution modeling of equilibrium/non-equilibrium phase-behavior. Chemical Engineering Science, 192, 371–379.

Cheng, C., Wang, F., Tian, Y., Wu, X., Zheng, J., Zhang, J., Li, L., Yang, P., Zhao, J., 2020. Review and prospects of hydrate cold storage technology. Renewable and Sustainable Energy Reviews, 117, 109492.

Fournaison, L., Delahaye, A., Chatti, I., Petitet, J.-P., 2004. CO2 Hydrates in Refrigeration Processes. Ind. Eng. Chem. Res., 43(20), 6521–6526.

Ge, B.-B., Zhong, D.-L., Lu, Y.-Y., 2019. Influence of water saturation and particle size on methane hydrate formation and dissociation in a fixed bed of silica sand. Energy Procedia, 158, 5402–5407.

Heeschen, K.U., Schicks, J.M., Oeltzschner, G., 2016. The promoting effect of natural sand on methane hydrate formation: Grain sizes and mineral composition. Fuel, 181, 139–147.

Kumar, A., Sakpal, T., Roy, S., Kumar, R., 2015. Methane hydrate formation in a test sediment of sand and clay at various levels of water saturation. Canadian Journal of Chemistry, 93(8), 874–881.

Li, G., Hwang, Y., Radermacher, R., 2012. Review of cold storage materials for air conditioning application. International Journal of Refrigeration, 35(8), 2053–2077.

Linga, P., Clarke, M.A., 2017. A Review of Reactor Designs and Materials Employed for Increasing the Rate of Gas Hydrate Formation. Energy Fuels, 31(1), 1–13.

Liu, W., Wang, Shanrong, Yang, M., Song, Y., Wang, Shenglong, Zhao, J., 2015. Investigation of the induction time for THF hydrate formation in porous media. Journal of Natural Gas Science and Engineering, 24, 357–364.

Malagar, B.R.C., Lijith, K.P., Singh, D.N., 2019. Formation & dissociation of methane gas hydrates in sediments: A critical review. Journal of Natural Gas Science and Engineering, 65, 168–184.

Marinhas, S., Delahaye, A., Fournaison, L., 2007. Solid fraction modelling for CO2 and CO2–THF hydrate slurries used as secondary refrigerants. International Journal of Refrigeration, 30(5), 758–766.

Mekala, P., Busch, M., Mech, D., Patel, R.S., Sangwai, J.S., 2014. Effect of silica sand size on the formation kinetics of CO2 hydrate in porous media in the presence of pure water and seawater relevant for CO2 sequestration. Journal of Petroleum Science and Engineering, 122, 1–9.

Nguyen, N.N., Galib, M., Nguyen, A.V., 2020. Critical Review on Gas Hydrate Formation at Solid Surfaces and in Confined Spaces—Why and How Does Interfacial Regime Matter? Energy Fuels, 34(6), 6751–6760.

Oya, S., Aifaa, M., Ohmura, R., 2017. Formation, growth and sintering of CO2 hydrate crystals in liquid water with continuous CO2 supply: Implication for subsurface CO2 sequestration. International Journal of Greenhouse Gas Control, 63, 386–391.

Pan, Z., Liu, Z., Zhang, Z., Shang, L., Ma, S., 2018. Effect of silica sand size and saturation on methane hydrate formation in the presence of SDS. Journal of Natural Gas Science and Engineering, 56, 266–280.

Qin, Y., Bao, R., Shang, L., Zhou, L., Meng, L., Zang, C., Sun, X., 2022. Effects of Particle Size and Types of Porous Media on the Formation and Occurrence of Methane Hydrate in Complex Systems. Energy Fuels, 36(1), 655–668.

Qin, Y., Pan, Z., Liu, Z., Shang, L., Zhou, L., 2021. Influence of the Particle Size of Porous Media on the Formation of Natural Gas Hydrate: A Review. Energy Fuels, 35(15), 11640–11664.

Sahu, C., Sircar, A., Sangwai, J.S., Kumar, R., 2022. Effect of sodium tripolyphosphate (STPP) and tetrasodium pyrophosphate (TSPP) on the formation kinetics of CO2 hydrate in bulk and porous media in the presence of pure water and seawater relevant for CO2 sequestration. International Journal of Greenhouse Gas Control, 114, 103564.

Wang, J., Zhang, L., Ge, K., Dong, H., 2021. Capillary pressure in the anisotropy of sediments with hydrate formation. Fuel, 289, 119938.

Wang, X., Zhang, F., Lipiński, W., 2020. Carbon dioxide hydrates for cold thermal energy storage: A review. Solar Energy, 211, 11–30.

Zhang, B., Zhou, L., Liu, Changling, Zhang, Q., Wu, Qiang, Wu, Qiong, Liu, Chuanhai, 2018. Influence of sediment media with different particle sizes on the nucleation of gas hydrate. Natural Gas Industry B, 5(6), 652–659.

Zhang, F., Wang, X., Wang, B., Lou, X., Lipiński, W., 2022. Effects of silica gel nanopores and surfactants on CO2 hydrate formation kinetics—An experimental and modeling study. Chemical Engineering Science, 118002.